Memoirs of the Faculty of Engineering and Design
Kyoto Institute of Technology 51 (March, 2003)

Notes on Surface Image Characteristic of Debris Flow

Hiroyuki INABA

(Received September 10, 2002 ; Accepted October 28, 2002)

Abstract

Nowadays, debris flows cause a lot of damage all over the world. The surface image of the flow, which is recorded by video recorder is one of the most important data in drawing a hazard map or constructing a sediment control dam. So far, authors have proposed an AR (Auto Regressive) type image model of a surface image of debris flow, and evaluate various measurement methods by using the artificial random image model. Since the parameters of the model is determined experimentally, it is not known that the artificial image exactly simulate the surface image of debris flow. In this paper, first we estimate the parameter of the image model by the least square error criterion from the real debris flow image. Second, we study some characters of the surface image of the debris flow such as particle size of the image, and isotropy of the image, etc. from the obtained model. As the result, we conclude that the particle size of the debris flow image is estimated correctly from our model in most cases, and the surface images of the many debris flows are not isotropic.

Key Words: *Debris flow; AR model; hazard map; image processing*

1. Introduction

A great deal of damage has been done by a debris flow in the world. Debris flow or flood flow can cause serious damage, including great loss of lives, houses, and land. If we can estimate the scale of the flow, the damage by the flow may decrease.

The surface image of debris flow or flood flow is random, but the all of the flow moves for roughly constant direction. The surface velocity of debris flow is one of the important physical parameters that are considered in drawing a hazard map or constructing a sediment control dam.

So far, many remote sensing measurement methods such as spatial filtering, laser-Doppler method, etc. have been proposed[1)~5)] and applied to the surface velocity measurement of debris flow[6)~8)]. Knowing the characteristic of the surface image is important for precise measurement in these methods.

In this paper, firstly, it is shown that an AR (Auto-Regressive) model of debris flow is determined from a video image of a real debris flow. Secondly, some of the characteristic of surface image of debris flow are analized from the model.

2. AR model of image

Generally, debris flow, flood flow or pyroclastic flow are called a random flow. In this paper, it is assumed that such a random flow is an homogeneous stochastic field. AR (Auto-Regressive) model is one of the good model to realize a stationary process.

A 2-dimensional AR representation for an image is determined by the following equation.

$$\hat{I}_{m,n} = \sum_k \sum_l a_{k,l} I_{m-k,n-l} + \beta W_{m,n} \qquad (1)$$

In the above equation, $I_{m,n}$ shows an brightness level of the pixel (m, n), and $a_{k,l}$ are coefficients for prediction, (k, l) is a coordinate in a prediction field. A prediction field is shown by Figure 1.

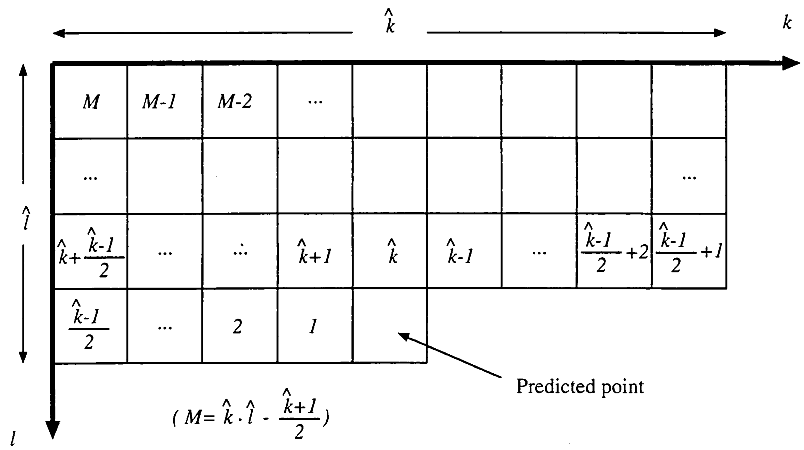

Fig. 1. Prediction field.

A noise term $W_{m,n}$ is white Gaussian noise, and the mean equal to zero.

$$< W_{m,n} W_{m',n'} > = \delta_{m,m'} \delta_{n,n'} \qquad (2)$$

The coefficients $a_{k,l}$ is determined by minimizing prediction error. The mean square prediction error is defined as

$$E_N = \frac{1}{N} \sum_{j=0}^{N-1} e_j^2$$
$$= \frac{1}{N} \sum_{m,n} \left(I_{m,n} - \sum_{k,l} a_{k,l} I_{m-k,n-l} \right)^2, \qquad (3)$$

where a parameter N is the number of samples.

For minimization of the error E_N, the following equations

$$\frac{\partial E_N}{\partial a_{k,l}} = 0 \tag{4}$$

are given. The set of the equations is a simultaneous system of linear equations, where the coefficients are formed by autocorrelation of the samples.

For the sake of consideration in the following section, we introduce two-dimensional homogeneous stochastic field $I_{m,n}$ determind by the following differential eq. (5)[9].

$$I_{m+1,n}+I_{m-1,n}+I_{m,n+1}+I_{m,n-1}-(4+K^2)I_{m,n} = CW_{m,n}, \tag{5}$$

where K is a spatial correlation parameter. A spatial correlation is more strong for less K.

A power spectrum density function of $I_{m,n}$ defined by eq. (5) is shown as

$$S(\lambda, \mu) = \frac{C^2}{4\pi|e^{i\lambda}+e^{-i\lambda}+e^{i\mu}+e^{-i\mu}-4-K^2|^2} \tag{6}$$

$$(-\pi \leq \lambda, \mu \leq \pi).$$

The coefficients of AR model for the field $I_{m,n}$ can be calculated by a quasi-isomorphic transformation[9].

3. Model of debris flow

In this section, some AR model of debris flow are constructed from video images of real debris flow by the method of the previous section.

The video image records debris flow occurred at Mt.Yakedake Kamikamihorisawa in Japan on Aug. 6, 2000. Three samples are used from the video image. The recorded time for each samples are the following.

- Surface image of debris flow (Sample A) PM 1:57:42
- Surface image of debris flow (Sample B) PM 1:58:00
- Surface image of debris flow (Sample C) PM 1:58:18

Figures 3, 5 and 7 show the value of prediction coefficient for sample A, B, and C. In these figures, indices of coefficients are labeled like Fig. 1.

The degree M of prediction for each sample is as follows. The optimized degree by FPE(Final Prediction Error) criterion is searched for various $\hat{k}$ and $\hat{l}$ in Fig. 1.

- Sample A Degree $M = 283$ $(\hat{k} = 27, \hat{l} = 11)$
- Sample B Degree $M = 333$ $(\hat{k} = 29, \hat{l} = 12)$
- Sample C Degree $M = 237$ $(\hat{k} = 25, \hat{l} = 10)$

Figures 2(a), 4(a) and 6(a) show the image of sample A, B and C, and Figs. 2(b), 4(b) and 6(b) show the synthetic image by using AR model's parameters estimated from each sample. Comparing with these figures, we can observe that the 'part icle size' of the synthetic image is almost same for the original sample image.

For predictive coefficients, each of label No. 1 and No. 27 for sample A, label No. 1 and No. 29 for sample B, and label No. 1 and No. 25 for sample C have large value. These labels correspond to the left neighbor and the upper neighbor of the predictive point each other.

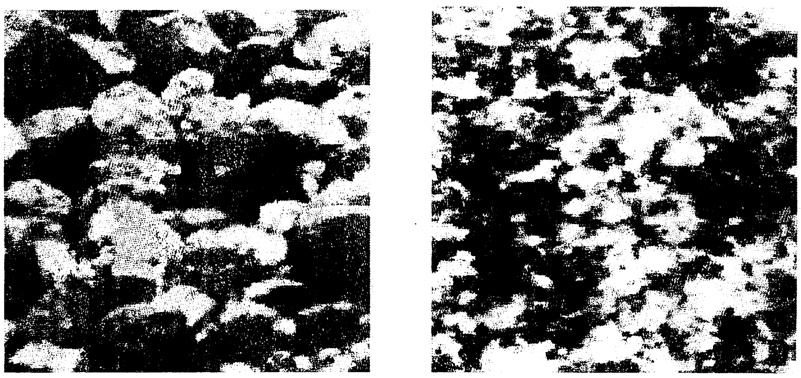

(a)Debris flow. (b)Synthetic image.

Fig. 2. Surface image of debris flow and synthetic image (Sample A).

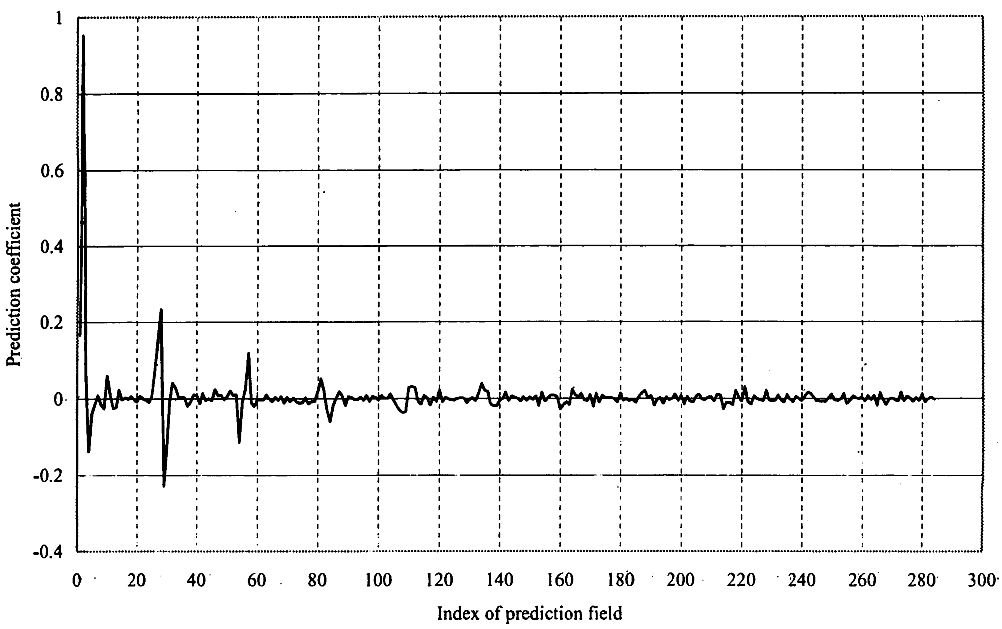

Fig. 3. Predictive coefficients of AR model (Sample A).

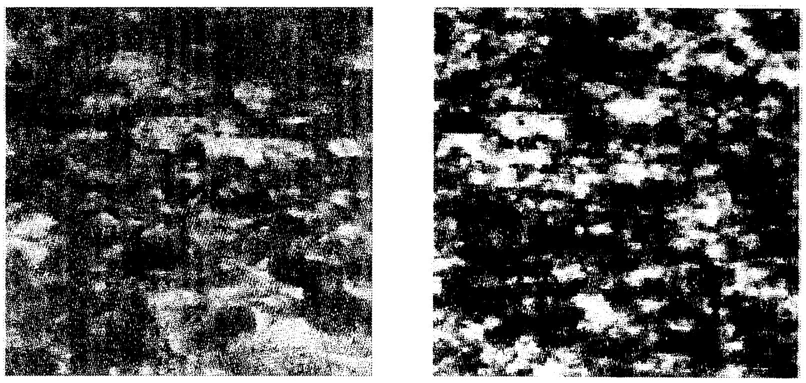

(a)Debris flow. (b)Synthetic image.

Fig. 4. Surface image of debris flow and synthetic image (Sample B).

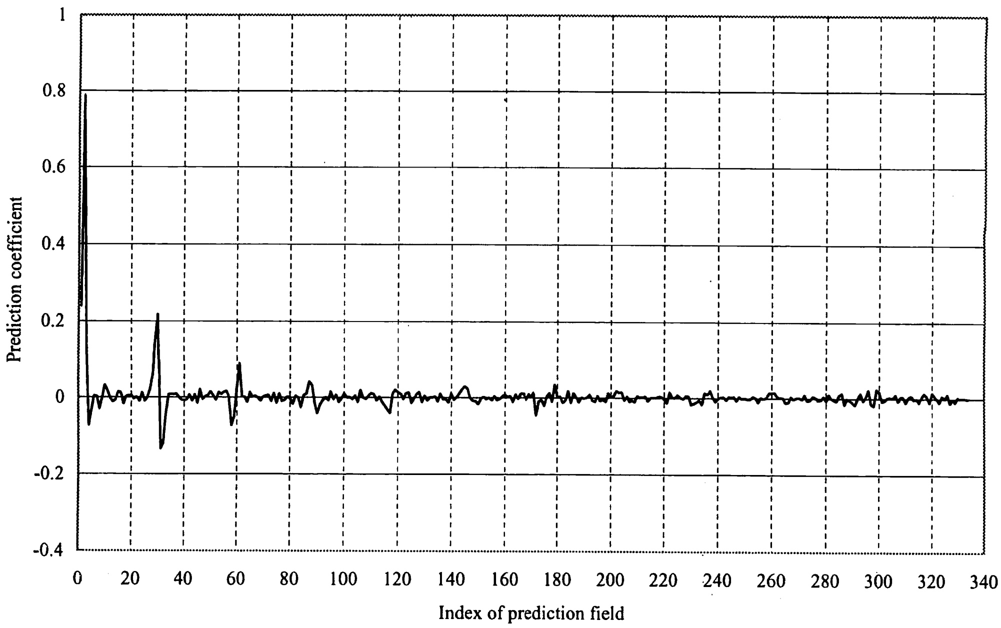

Fig. 5. Predictive coefficients of AR model (Sample B).

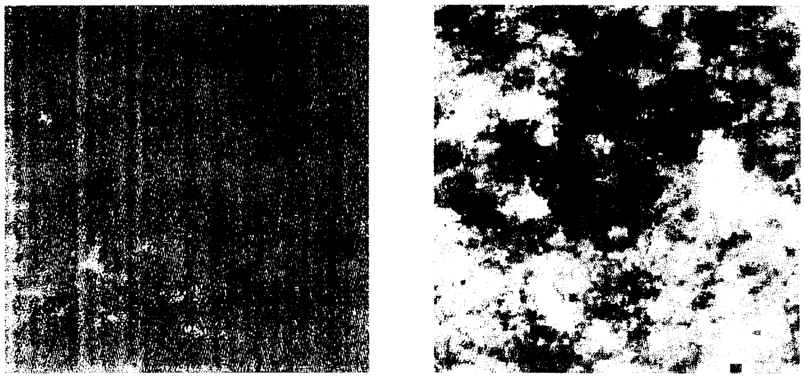

(a)Debris flow. (b)Synthetic image.

Fig. 6. Surface image of debris flow and synthetic image (Sample C).

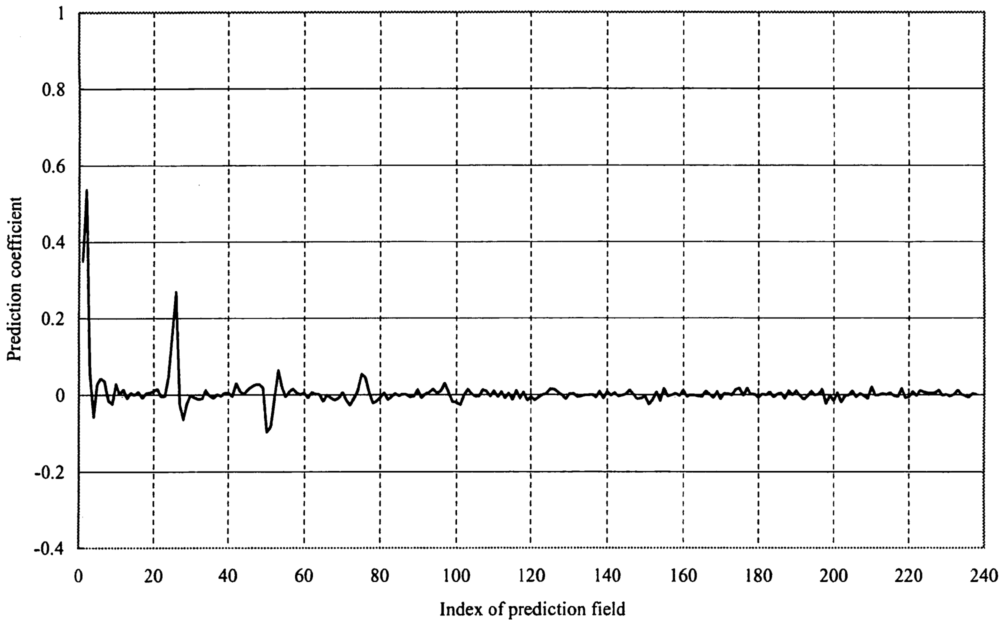

Fig. 7. Predictive coefficients of AR model (Sample C).

4. Consideration

4.1 Spatial correlation of debris flow

Figures 8, 9 and 10 show the normalized autocorrelation of original image and synthetic image for sample A, B and C each other.

In these figures, each of the dotted lines is the reference line for correlation parameter $K = 0.1, 0.2, 0.3, 0.4$ defined in eq. (5). Table 1 shows the correlation parameter K estimated from Figs. 8, 9 and 10, and also shows an error between original image's K and synthetic image's K (See Appendix).

Table. 1. Estimated autocorrelation parameter K.

		Original	Synthetic	Error rate
Sample A	m	0.10	0.10	0%
	n	0.22	0.23	7.13%
Sample B	m	0.15	0.16	7.34%
	n	0.29	0.32	11.62%
Sample C	m	0.15	0.19	33.2%
	n	0.16	0.22	41.9%

In Figs. 8 and 9, both of the autocorrelation function for original image and synthetic image have almost similar trend. Furthermore, error rate for sample A and B in Table 1 is considerably small. It is considered that the estimation for sample A and B are successfully done.

However, each of the autocorrelation function for original image and synthetic image for sample C has different trend in Fig. 10. Also error rate is not so small in Table 1. Namely, the estimation for sample C is not so accurate.

In Table 1, autocorrelation parameter K for sample B is larger than that for sample A. Generally, a larger value of K means a smaller particle size of surface pattern. This result agrees with subjective impression for Figs. 2 and 4. However, the estimated value of K for sample C is less than that for sample B for almost case in Table 1. The result contradicts subjective impression for Figs. 4 and 6 (The particle size for sample C is considerably smaller than that for sample B).

One explanation for this result may be considered that a cluster consisted of some small particles is recognized as a larger particle when a particle size is so small like sample C.

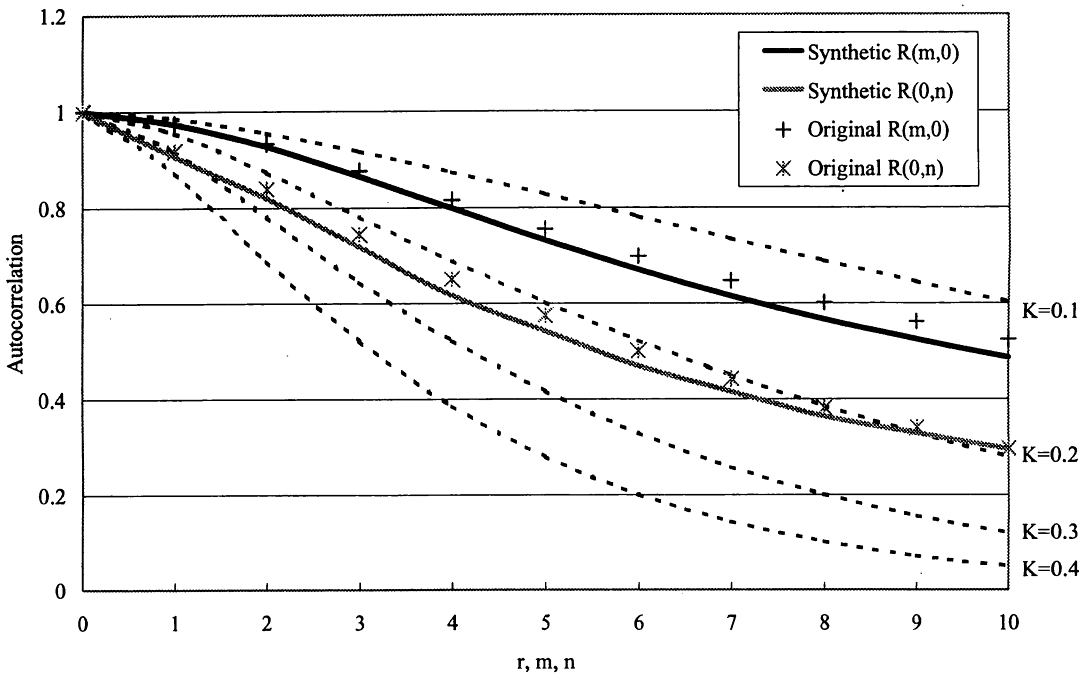

Fig. 8. Autocorrelation for original and synthetic image (Sample A).

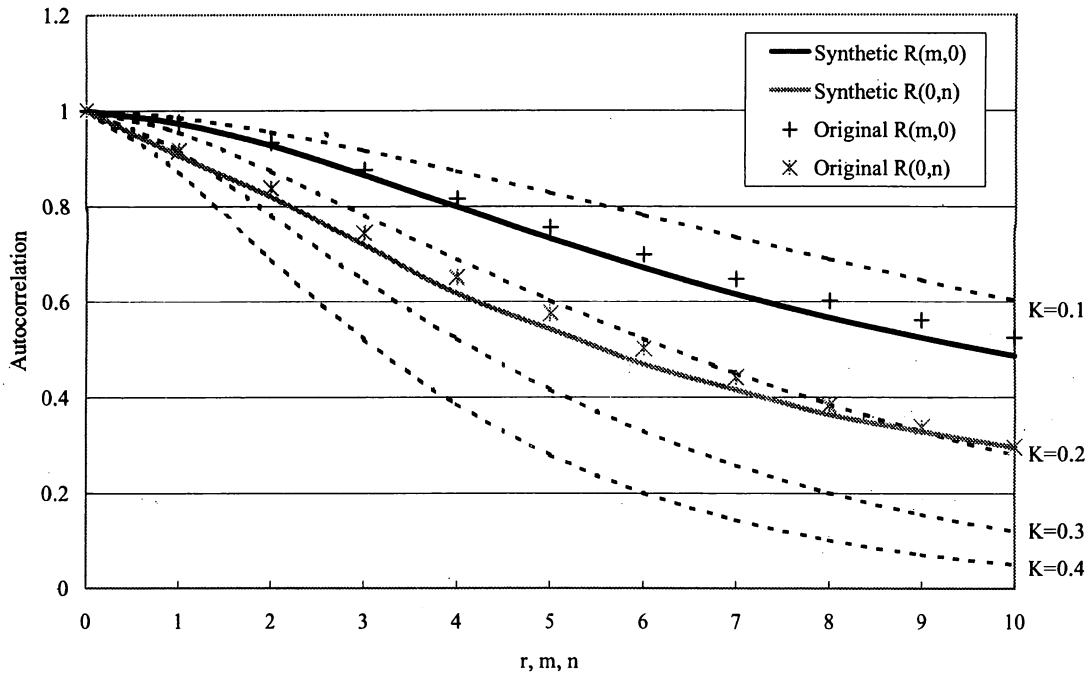

Fig. 9. Autocorrelation for original and synthetic image (Sample B).

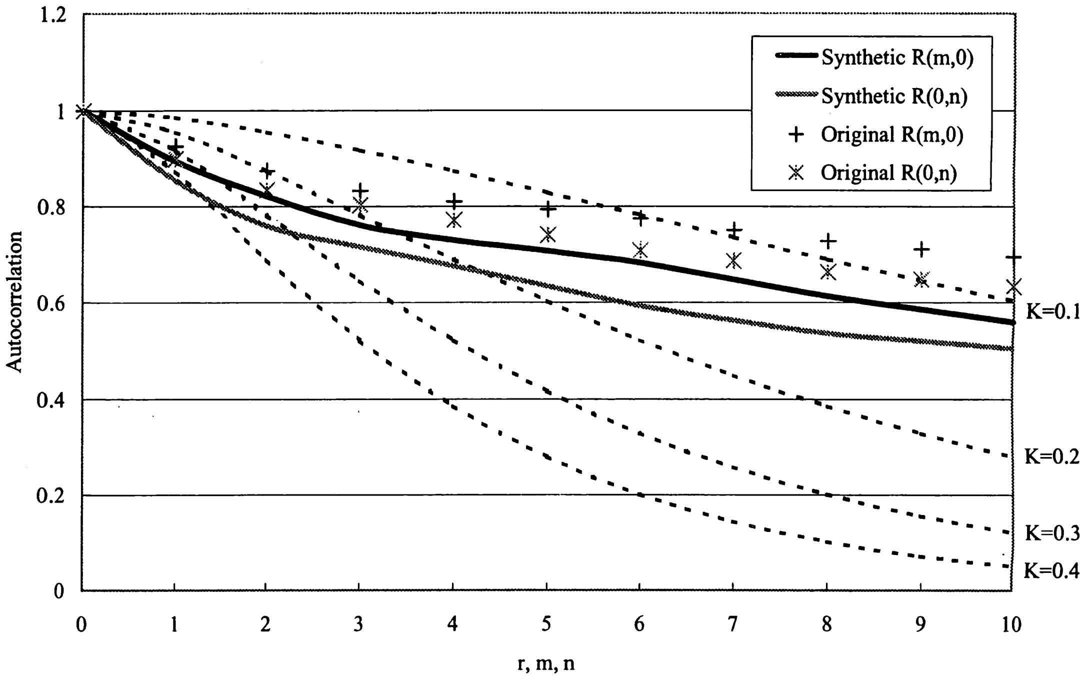

Fig. 10. Autocorrelation for original and synthetic image (Sample C).

4.2 Spatial isotropy of debris flow

Figures 11(a), 13(a) and 15(a) are the figures of debris flow rotated to the right at 90 degree, and the Figs. 12, 14 and 16 are the predictive coefficients of the rotated images for the index of predictive field less than 10. Figures 11(b), 13(b) and 15(b) are the synthetic images by using the predictive coefficients.

We can see that a characteristic of debris flow between the rotated and the original is partially different from these graphs. Especially for sample A and B, the difference is larger than sample C. The property is also confirmed from Figs. 8, 9 and 10. The autocorrelation $R(m, 0)$ for horizontal and the autocorrelation $R(0, n)$ for vertical is rather different for sample A and B, but, it is not so different for sample C.

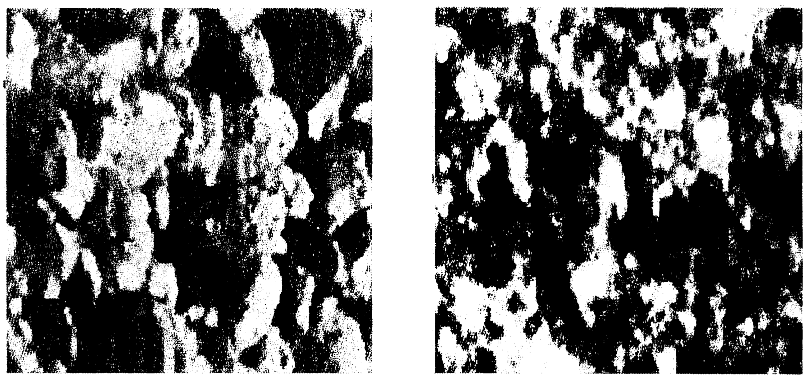

(a)Debris flow. (b)Synthetic image.

Fig. 11. Surface image of debris flow rotated at 90 degree and synthetic image (Sample A).

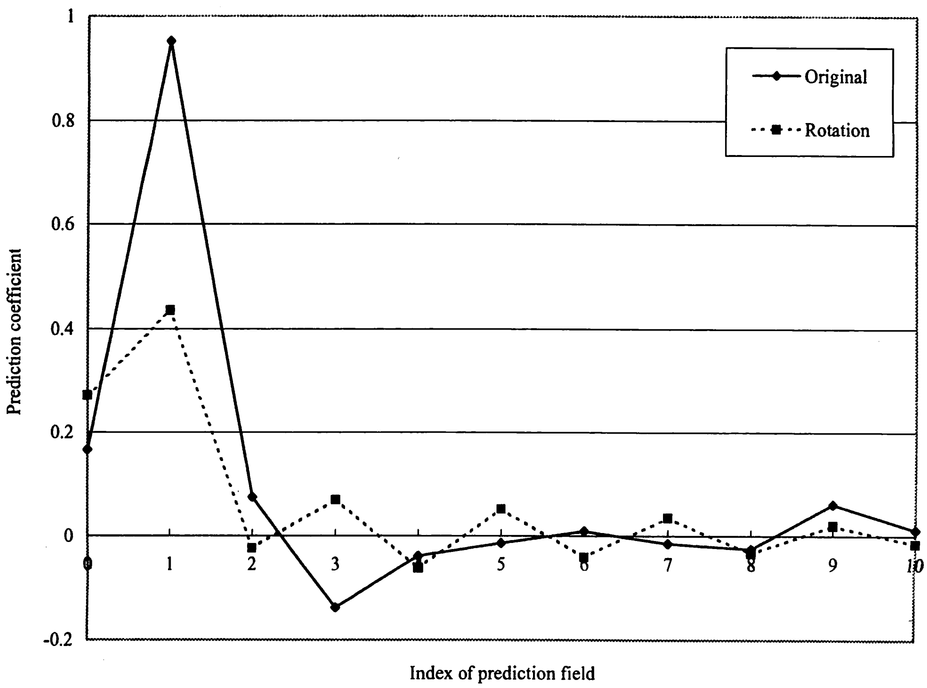

Fig. 12. Predictive coefficients of AR model after rotation (Sample A).

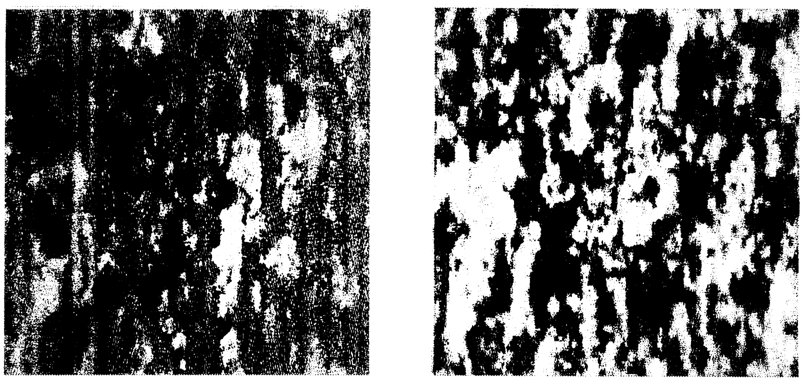

(a)Debris flow. (b)Synthetic image.

Fig. 13. Surface image of debris flow rotated at 90 degree and synthetic image (Sample B).

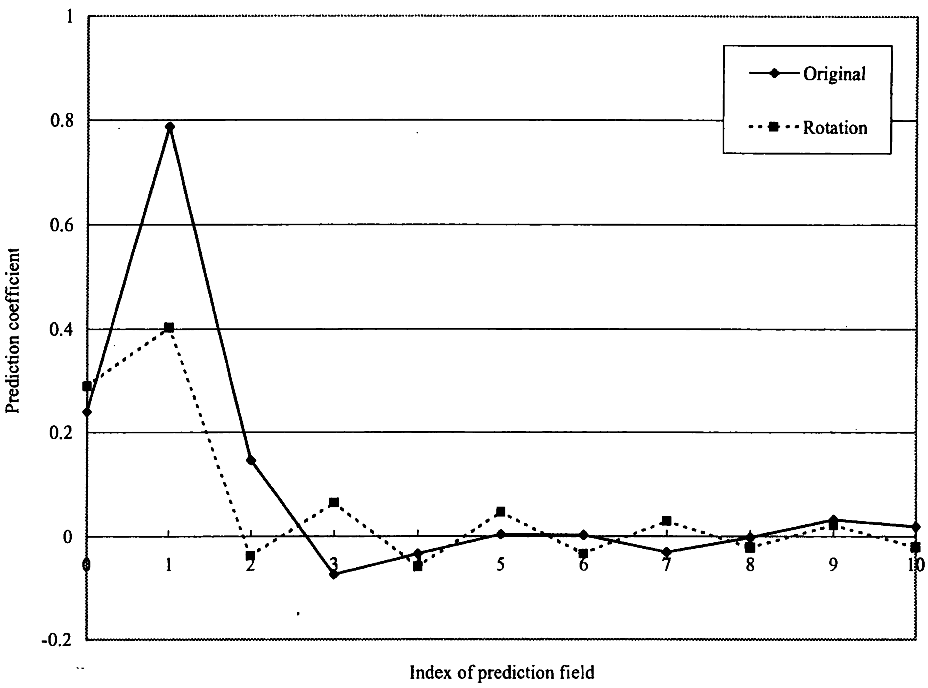

Fig. 14. Predictive coefficients of AR model after rotation (Sample B).

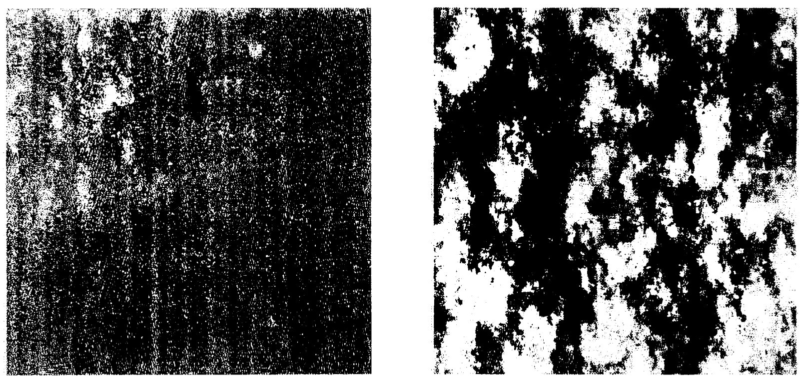

(a)Debris flow. (b)Synthetic image.

Fig. 15. Surface image of debris flow rotated at 90 degree and synthetic image (Sample C).

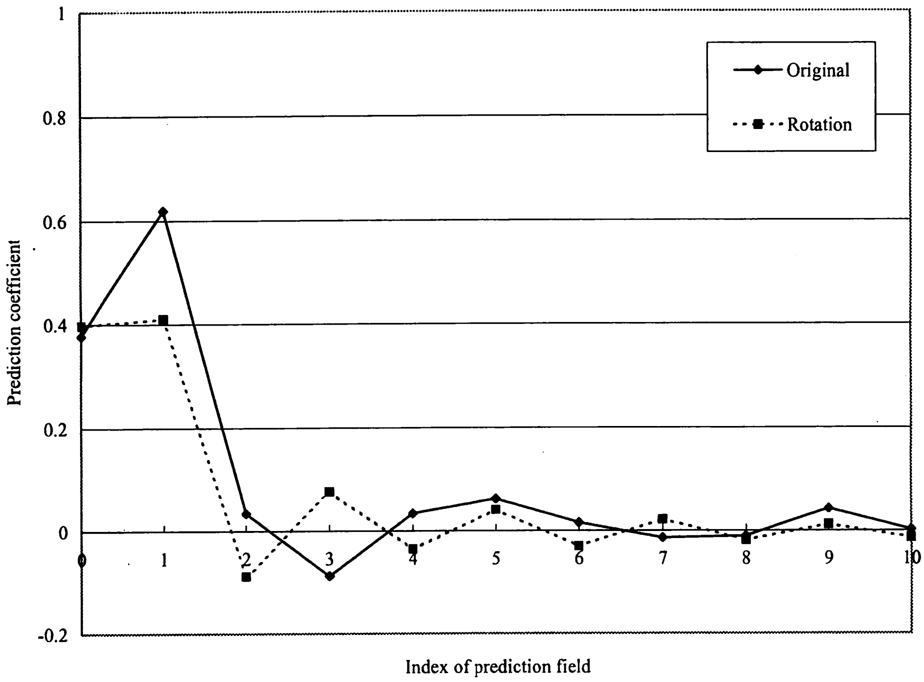

Fig. 16. Predictive coefficients of AR model after rotation (Sample C).

5. Conclusion

In this paper, it is shown that a surface image of debris flow digitized from a video image can be expressed by AR model for the most case. Since a synthetic image generated from the AR model has almost similar characteristic of the original debris flow image, we can use the generated image as an artificial debris flow image. It is also shown that a particle size of debris flow is calculated from the AR model.

An optimized degree of the AR model in FPE criterion is about 300. The degree is too many, but a basic characteristic of the image can be studied from the top of 30 coefficients.

In case a particle size of debris flow is so small (it is almost considered as a mud flow), the estimated correlation parameter is not so accurate.

For spatial isotropy of debris flow, we can conclude that some surface image of debris flow has a different characteristic of the image for the direction. So far, a spatially isotropic model is used for debris flow, we may consider a non-isotropic type for more accurate model of debris flow in future.

It is expected that the result of this paper may contribute to a more effective disaster prevention such as drawing hazard map or designing a new observation system for debris flow.

Acknowledgments

The author would like to express special thanks to Prof. Yasuo Yoshida of Kyoto

Institute of Technology and Prof. Yasumasa Itakura of Shiga University for their kind suggestion, and Ms. Kaori Yamaguchi for valuable discussion and computer simulation throughout the work reported in this paper.

The video image of debris flow is offered from Dr. Hiroshi Suwa of Kyoto University and the Matsumoto Erosion Control Works of the Ministry of Construction. The author also thanks for their cooperation.

Dept. of Electronics and Information Science
Faculty of Engineering and Design,
Kyoto Institute of Technology
Goshokaido-cho, Matsugasaki, Sakyo-ku, Kyoto 606-8585

References

1) J. T. Ator, *J. Opt. Soc. Am.*, **53**, 1416-1422, (1963).
2) Yeh, Y. and Cummins, H. Z, *Appl. Phys. Lett.* **4**, 176, (1964).
3) Itakura, Y., Sugimura, A. and Tsutsumi, S., *Applied Optics*, **20**, 16, 2819-2826, (1981).
4) Itakura, Y., Takeuchi, M, Kasahara, M. and Ogura, H., *Proc. 1989 Int. Symp. on Noise and Clutter Rejection in Radars and Imaging Sensors,* 148-153, (1989).
5) Honda, M., Inaba, H., Itakura, Y. and Kasahara, M., *Proc. 1994 Int. Symp. on Noise and Clutter Rejection in Radars and Imaging Sensors,* 223-228, (1994).
6) Itakura, Y., Ogawa, K., Suwa, H. and Mizuhara, K., *Proc. Int. Symp. on Fluid Control and Measurement,* Tokyo, 781-786, (1985).
7) Itakura, Y. and Suwa, H., *Proc. The Japan-China Symp. on Landslides and Debris Flows,* Japan, 199-204, (1989).
8) Itakura, Y., Inaba, H. and Kasahara, M., *Proc. IMEKO World Congress,* **3**, 2086-2091, (1994).
9) Y. Yoshida, H. Ogura and S. Sakura, Trans. on Electronics and Communications of IEICE, **65-A**, 5, 1-10, (1982).

Appendix

The correlation parameter K of debris flow image in Table 1 are estimated in the following manner.

The autocorrelation function of the stochastic field defined by eq. (5) is

$$R_p(r,\ K) = \sigma^2 KrK_1(kr)\ , \tag{7}$$

where $K_n(x)$ is modified second kind Bessel function with degree n, and $\sigma^2 = R_p(0, K)$.

On the other hand, autocorrelation function of debris flow image is defined by $R\ (m,\ n) = \langle I_{k,l} I_{k+m,l+n} \rangle$, and the normalized autocorrelation function is given as $\hat{R}(m,\ n) = R(m,\ n)/R(0,\ 0)$.

For the estimation of the parameter K, first we calculate the value K_m from the following equation:

$$K_m = \min_K |\hat{R}(m,\ 0) - \hat{R}_p(m,\ K)| \tag{8}$$

for $m = 1, 2, \cdots\cdots, 10$.

Then the correlation parameter K is estimated by the following weighted sum of K_ms.

$$K = \sum_{m=1}^{10} K_m \frac{\hat{R}(m,\ 0)}{\sum_{m=1}^{10} \hat{R}(m,\ 0)}\ . \tag{9}$$